受入
79-11-349
高工研図書室

EUROPEAN ORGANIZATION FOR NUCLEAR RESEARCH

CERN-EP/79-107
26 September 1979

FIRST MEASUREMENT OF THE Ω^- DECAY BRANCHING RATIOS

Bristol[1)]-Geneva[2)]-Heidelberg[3)]-Orsay[4)]-
Rutherford[5)]-Strasbourg[6)] Collaboration

M. Bourquin[2)], R.M. Brown[5)], Y. Chatelus[6)], J.C. Chollet[4)],
A. Degré[6)], D. Froidevaux[4)], A.R. Fyfe[1)], J.-M. Gaillard[4)],
C.N.P. Gee[5)], W.M. Gibson[1)], P. Igo-Kemenes[3)], P.W. Jeffreys[1)],
B. Merkel[4)], R. Morand[6)], H. Plothow[*)], J.-P. Repellin[4)],
B.J. Saunders[5)], G. Sauvage[4)], B. Schiby[6)], H.W. Siebert[3)],
V.J. Smith[1)], K.-P. Streit[3)], R. Strub[6)], J.J. Thresher[5)]
and S.N. Tovey[**)]

ABSTRACT

In an experiment in the CERN-SPS charged-hyperon beam, the main Ω^- decay branching ratios have been measured to be

$$\Gamma(\Omega^- \to \Lambda K^-)/\Gamma(\text{all}) = 0.686 \pm 0.013$$

$$\Gamma(\Omega^- \to \Xi^0\pi^-)/\Gamma(\text{all}) = 0.234 \pm 0.013$$

$$\Gamma(\Omega^- \to \Xi^-\pi^0)/\Gamma(\text{all}) = 0.080 \pm 0.008 \ .$$

The relative branching ratio of the two $\Xi\pi$ modes provides a test of the $\Delta I = 1/2$ rule in decuplet-octet transitions.

A search has also been made for the rare decay modes $\Omega^- \to \Lambda\pi^-$, $\Omega^- \to \Xi^-\gamma$, $\Omega^- \to \Xi^-\pi^+\pi^-$ and $\Omega^- \to \Xi^0 e^-\bar{\nu}$.

(Submitted to Physics Letters)

1) H.H. Wills Physics Laboratory, University of Bristol, England.

2) University of Geneva, Switzerland.

3) Physikalisches Institut, Universität Heidelberg, Germany.
Work supported by the Bundesministerium für Forschung und Technologie, Germany.

4) Laboratoire de l'Accélérateur Linéaire, Orsay, France.

5) Rutherford Laboratory, Chilton, Didcot, England.

6) CRN - Division des Hautes Energies, Strasbourg, France.

*) CERN, Geneva, Switzerland.

**) University of Melbourne, Australia, and CERN, Geneva, Switzerland.

1. INTRODUCTION

This article presents a measurement of Ω^- decay branching ratios from the analysis of data taken in 1978 with the CERN-SPS charged-hyperon beam. The measurement of the $\Omega^- \to \Xi^0\pi^-/\Omega^- \to \Xi^-\pi^0$ relative branching ratio provides the first test of the $\Delta I = \frac{1}{2}$ rule for decuplet-octet transitions. Prior to this experiment, no quantitative results on Ω^- branching ratios have been reported.

Preliminary results, based on two-thirds of the data, were reported at the Tokyo Conference [1] and a measurement of the Ω^- lifetime using the full sample has been published recently [2]. Descriptions of the hyperon beam [3] and the apparatus used for the Ω^- measurements [2] have already been given and are not repeated here.

In sections 2 and 3 we describe the method of event selection and the branching ratio determination for the principal decay modes $\Omega^- \to \Lambda K^-$, $\Omega^- \to \Xi^0\pi^-$, and $\Omega^- \to \Xi^-\pi^0$. In section 4 we discuss the rare decay modes $\Omega^- \to \Lambda\pi^-$, $\Omega^- \to \Xi^-\gamma$, $\Omega^- \to \Xi^-\pi^+\pi^-$ and $\Omega^- \to \Xi^0 e^-\bar{\nu}$.

2. EVENT SELECTION

In this and the following section we will discuss the decay modes :

$$\Omega^- \to \Lambda K^-, \quad \Lambda \to p\pi^-$$

$$\Omega^- \to \Xi^0\pi^-, \quad \Xi^0 \to \Lambda\pi^0, \quad \Lambda\pi^0 \to p\pi^-$$

$$\Omega^- \to \Xi^-\pi^0, \quad \Xi^- \to \Lambda\pi^-, \quad \Lambda\pi^- \to p\pi^- .$$

As described elsewhere [2] a DISC Čerenkov counter at the exit of the magnetic channel is used to trigger on Ω^-. The charged decay products are analysed in a magnetic spectrometer. Gamma-rays which pass through the aperture of the spectrometer magnet are detected by an array of lead-glass counters, and large-angle γ-rays by a combination of a lead converter and a scintillator hodoscope which was placed upstream of the magnet. Data were taken at two hyperon beam momenta, 98.5 GeV/c and 115 GeV/c.

In all these final states there are three charged particles, namely a proton and a π^- from Λ decay and an additional π^- or K^-. Thus, as described in ref. 2, the requirements of more than one charged decay particle in a scintillation counter placed upstream of the spectrometer, and of a high momentum positive particle ("proton") in a scintillation counter placed downstream of the spectrometer completed the trigger conditions.

2.1 Selection criteria common to all decay modes

We required the pulse height in the scintillation counter at the downstream end of the DISC (counter T in fig. 1 of ref. 2) to be less than twice the mean pulse height for a single particle, since an important source of triggers consisted of $\Xi^- \to \Lambda\pi^-$, $\Lambda \to p\pi^-$ cascades, which occurred upstream of the DISC or within it and where the combined Čerenkov light from several particles simulated an Ω^- signal.

In the $\Xi\pi$ modes, knowledge of the beam track is necessary to reconstruct the Ω^- decay vertex. To avoid possible biases due to early Ω^- decays, we used for all decays a minimum requirement for a beam track, defining it by a space point in beam chambers upstream of the DISC and by the mean beam direction.

We also required a $\Lambda \to p\pi^-$ decay, i.e. a positive and a negative track which extrapolated to a vertex located between z = 2 m and z = 13.5 m, where z is the coordinate along the beam. The plane at z = 2 m is 0.8 m before the end of the sensitive volume of the DISC and z = 13.5 m is the position of the first drift chamber of the spectrometer (see fig. 1 of ref. 2). The invariant mass

$m_{p\pi}$ was required to be within ±10 MeV/c^2 of the Λ mass. The observed width of the $m_{p\pi}$ distribution was 4 MeV/c^2 (FWHM).

2.2 $\Omega^- \to \Lambda K^-$ selection

For this decay mode we required a negative track which intersected the reconstructed Λ track to give an Ω^- vertex located at $z_\Omega > 2$ m and, within errors, upstream of the Λ vertex. Assuming the negative track to be a K^-, we calculated the invariant mass $m_{\Lambda K}$ and required it to be within ±50 MeV/c^2 of the Ω^- mass.

Cuts were also applied to the difference $\Delta\vec{p}$ between the mean beam momentum $\vec{p}_{beam}$ and the combined momentum of the charged decay particles. The component transverse to the beam, Δp_T, had to be less than 0.14 GeV/c and the component parallel to the beam, Δp_L, had to be less than 10 GeV/c in magnitude. The r.m.s. deviations of these quantities for $\Omega^- \to \Lambda K^-$ were $\delta p_T = 0.04$ GeV/c and $\delta p_L = 0.035\, p_{beam}$. To identify the $\Xi^- \to \Lambda\pi^-$ background, we also computed the invariant mass $m_{\Lambda\pi}$, assuming the negative track to be a π^-. Figure 1a shows the plot of $m_{\Lambda K}$ versus $m_{\Lambda\pi}$ for the selected events at 98.5 GeV/c.

Clearly, a large number of Ξ^- decays is contained in this sample. The band of background events below the Ξ^- mass band is attributed to spurious track combinations caused by early Ξ^- decays or interactions in the magnetic channel. An additional cut $m_{\Lambda\pi} > 1.35$ GeV/c^2 reduced both backgrounds to a negligible level.

Figure 1b shows the $m_{\Lambda K}$ distribution after this cut. The observed width is 6 MeV/c^2 (FWHM). Within ±10 MeV/c^2 of the Ω^- mass, the sample contains 1208 (712) $\Omega^- \to \Lambda K^-$ events at 98.5 (115) GeV/c and an estimated background of 10 (7) events.

2.3 $\Omega^- \to \Xi^0\pi^-$ selection

We required a beam track and a negative particle track to give an Ω^- vertex located downstream of z = 2 m and, within errors, upstream of the Λ vertex. The Ω^--π^- missing mass was required to be within ±100 MeV/c^2 of the Ξ^0 mass. Background $\Xi^- \to \Lambda\pi^-$ decays were rejected by requiring that no combination of spectrometer tracks had a reconstructed mass $m_{\Lambda\pi} < 1.35$ GeV/c^2.

At this stage most of the background consisted of $\Omega^- \to \Lambda K^-$ decays, as shown by fig. 2, which is a scatter plot of the $(\Omega^- - \pi^-)$ missing mass versus the effective ΛK^- mass. The $\Omega^- \to \Lambda K^-$ events have on average a missing longitudinal momentum $\Delta p_L = 0$. They were removed by requiring $\Delta p_L > 0.06\ p_{beam}$. This cut also removed 12% of the genuine $\Omega^- \to \Xi^0\pi^-$ decays. The distribution of m_x^2, the square of the missing mass between the Ξ^0 and the Λ, is shown in fig. 3a for the remaining events. A clear peak centred at $m_x^2 = m_{\pi^0}^2$ is observed. In addition we required $-0.03\ GeV^2/c^4 < m_x^2 < 0.06\ GeV^2/c^4$. The distribution of the $(\Omega^- - \pi^-)$ missing mass after this cut is shown in fig. 3b. Within $\pm 20\ MeV/c^2$ of the Ξ^0 mass there are 215 (122) events at 98.5 (115) GeV/c.

Both the decay cascades $\Omega^- \to \Xi^0\pi^-$, $\Xi^0 \to \Lambda\pi^0$ and $\Omega^- \to \Xi^-\pi^0$, $\Xi^- \to \Lambda\pi^-$ have among the decay products a π^0 which decays into two γ-rays. There was a high probability for at least one of the γ-rays to be detected in either the lead-glass array or the lead/scintillator hodoscope. On the other hand, background events had a relatively low probability of giving a spurious γ-ray signal. Information from the γ-ray detectors was therefore used to estimate the background and the signal for each of the two decay modes.

The γ-ray detection efficiency was determined to be $\varepsilon_\gamma = 0.92 \pm 0.03$ for the $\Omega^- \to \Xi^0\pi^-$ decay using the data themselves according to the procedure described below. This efficiency was consistent with a value obtained from $\Sigma^+ \to p\pi^0$ data taken with the beam tuned to positive polarity. The fraction of background events which gave a spurious γ-ray signal was determined to be $r = 0.25 \pm 0.03$ using a restricted part of the $\Omega^- \to \Xi^-\pi^0$ sample which was known to contain only background events.

The small background in the Ξ^0 mass region was assumed to be given by a linear interpolation of the background in the regions on either side of the peak. Four equations were constructed using the observed number of events inside and outside the Ξ^0 mass region and with and without detected γ-rays. These four equations enabled us to determine the following four quantities: the signal in

the peak, the background, the γ-ray detection efficiency and the fraction of signal outside the peak. The results are a signal of 198 ± 15 (119 ± 11) $\Omega^- \to \Xi^0\pi^-$ events at 98.5 (115) GeV/c above a background of 17 (3) events. The γ-ray detection efficiencies obtained at both momenta agreed well with each other, their mean value being $\varepsilon_\gamma = 0.92 \pm 0.03$. Since most of the events in the peak region are signal and most of the events in the tails are background, the values obtained for the signal and for the γ-ray efficiency are insensitive to the exact value of r. Changing r by ±0.06 changes the total number of $\Omega^- \to \Xi^0\pi^-$ events by ±1.5.

2.4 $\Omega^- \to \Xi^-\pi^0$ event selection

The Ξ^- produced in this decay were selected in a similar way to $\Omega^- \to \Lambda K^-$ candidates. We required a negative track and the reconstructed Λ track to have an intersection located within errors downstream of z = 2 m and upstream of the Λ vertex. The $\Lambda\pi^-$ invariant mass was required to be within ±20 MeV/c^2 of the Ξ^- mass, the width of the $m_{\Lambda\pi}$ distribution being 6 MeV/c^2 (FWHM). The Ω^- vertex was reconstructed from the beam track and the reconstructed Ξ^- track, and this vertex was required to be downstream of z = 2 m.

The π^0 momentum was defined as the difference $\Delta\vec{p}$ between the mean beam momentum and the Ξ^- momentum. In fig. 4a we show a scatter plot of the longitudinal component Δp_L versus m_x^2, the square of the missing mass between the Ω^- and the Ξ^-. The plot contains the 98.5 GeV/c data. There is a prominent background from $\Xi^- \to \Lambda\pi^-$ decays which lies on a smooth curve with a maximum at $\Delta p_L = 0$, corresponding to Ξ^- with the nominal beam momentum. A second maximum at $\Delta p_L = 20$ GeV/c corresponds to Ξ^- of 78 GeV/c. Low-momentum Ξ^- cannot come directly from the target and are thought to be produced by Ω^- decaying in the channel or by particles interacting in the channel walls. The direction of some of these slow Ξ^- is within the acceptance of the DISC (±1.5 mrad). They constitute a very small fraction of the total beam; however those Ξ^- which have a momentum close to 78 GeV/c have the same velocity as Ω^- with the nominal beam momentum and thus trigger the DISC with high efficiency. The requirement of a γ-signal scales down this background by a factor r = 0.25 ± 0.03.

A cut was applied to the component of $\Delta\vec{p}$ transverse to the beam, removing events with $\Delta p_T < 0.15$ GeV/c, in particular those events where the Ξ^- contributed to the DISC signal. Since the c.m. momentum of the $\Omega^- \to \Xi^-\pi^0$ decay is 0.29 GeV/c, this cut removes only 16% of the genuine events. A further cut was made on Δp_L as indicated in fig. 4a, corresponding to $\Delta p_L > 0.12\ p_{beam}$ at $m_x^2 = 0$. In fig. 4b we show the distribution of m_x^2 after these two cuts for the 98.5 GeV/c data. The shaded events are those without a γ-signal. In the interval $-0.03\ \mathrm{GeV}^2/c^4 < m_x^2 < 0.06\ \mathrm{GeV}^2/c^4$ the sample contains 133 (65) events at 98.5 (115) GeV/c, of which 34 (13) have no γ-signal.

We calculate the γ detection efficiency for our $\Omega^- \to \Xi^-\pi^0$ samples from the value determined using $\Omega^- \to \Xi^0\pi^-$, taking into account the differences between the π^0 energy spectra and geometrical acceptances in the two cases. The result is $\varepsilon_\gamma = 0.95 \pm 0.03$. From this and from the background rejection factor $r = 0.25 \pm 0.03$ we obtain a signal of 94 ± 12 (51 ± 8) $\Omega^- \to \Xi^-\pi^0$ events at 98.5 (115) GeV/c.

3. ΛK AND Ξπ BRANCHING RATIOS

The acceptances for the different decay modes listed in table 1 were obtained by a Monte Carlo calculation. They were normalized to the flux of Ω^- which reach z = 1.7 m (approximately the centre of the DISC).

Systematic errors in the acceptances are important only if they are different for the various decay modes. In the acceptance ratio $\alpha = a_{\Lambda K}/a_{\Xi\pi}$ they originate from the following sources (the numbers are given for 98.5 GeV/c and also in brackets for 115 GeV/c).

Most of the decay particles passed through all four drift chambers downstream of the spectrometer magnet; however a small part of the acceptance was covered by only three chambers. The fraction of particles traversing three chambers was different for the $\Omega \to \Xi\pi$ and $\Omega \to \Lambda K$ modes and thus there was a small difference between the track-finding efficiencies in the two cases. This introduces an uncertainty $\delta\alpha/\alpha = \pm 1.3\%$ ($\pm 1.0\%$).

The uncertainties connected with the calculation of multiple scattering effects contribute $\delta\alpha/\alpha = \pm 0.6\%$ ($\pm 0.5\%$).

The calculation of the decrease of the DISC efficiency for Ω^- decays occurring inside the sensitive volume of the DISC, i.e. before z = 2.8 m, introduces an uncertainty $\delta\alpha/\alpha = \pm 0.5\%$ ($\pm 0.5\%$), owing to the different Ω^- decay point distributions for the final event samples.

Uncertainties in the positions of the beam trigger counter and beam halo veto counter (T and A in fig. 1 of ref. [2]) with respect to the beam axis result in a contribution $\delta\alpha/\alpha = \pm 0.6\%$ ($\pm 0.4\%$).

Finally, uncertainties in the measurement of the drift chamber efficiencies in the beam region give rise to $\delta\alpha/\alpha = \pm 0.5\%$ ($\pm 0.8\%$).

The total systematic error in the ratio of the acceptances for the ΛK and the $\Xi\pi$ decay modes is then $\delta\alpha/\alpha = \pm 1.7\%$ ($\pm 1.5\%$) at 98.5 (115) GeV/c.

The systematic error in the ratio of the $\Xi\pi$ acceptances, $\beta = a_{\Xi^0\pi^-}/a_{\Xi^-\pi^0}$, is smaller because these two decay configurations are very similar. From the same error sources we obtain the systematic error $\delta\beta/\beta = \pm 1.0\%$ at both momenta.

From the numbers of events derived in section 2 and from the calculated acceptances we obtain the branching ratios for each momentum separately, as listed in table 1. For this calculation we assume that the contributions from $\Omega^- \to \Lambda K^-$, $\Omega^- \to \Xi^0\pi^-$ and $\Omega^- \to \Xi^-\pi^0$ add up to 100% of the Ω^- decay rate. We also calculate the ratio $\Gamma(\Omega^- \to \Xi^0\pi^-)/\Gamma(\Omega^- \to \Xi^-\pi^0)$.

The branching ratios at 98.5 and 115 GeV/c are in good agreement. Averaging over the two momenta, we finally obtain

$$\frac{\Gamma(\Omega^- \to \Lambda K^-)}{\Gamma(\text{all})} = 0.686 \pm 0.013$$

$$\frac{\Gamma(\Omega^- \to \Xi^0\pi^-)}{\Gamma(\text{all})} = 0.234 \pm 0.013$$

$$\frac{\Gamma(\Omega^- \to \Xi^-\pi^0)}{\Gamma(\text{all})} = 0.080 \pm 0.008$$

$$\frac{\Gamma(\Omega^- \to \Xi^0\pi^-)}{\Gamma(\Omega^- \to \Xi^-\pi^0)} = 2.94 \pm 0.35 \ .$$

Using the Ω^- lifetime measured in the same experiment [2], $\tau_\Omega = (0.822 \pm \pm 0.028) \times 10^{-10}$ s, we obtain for the decay rates :

$$\Gamma(\Omega^- \to \Lambda K^-) = (0.835 \pm 0.033) \times 10^{10}\ s^{-1}$$

$$\Gamma(\Omega^- \to \Xi^0\pi^-) = (0.285 \pm 0.019) \times 10^{10}\ s^{-1}$$

$$\Gamma(\Omega^- \to \Xi^-\pi^0) = (0.097 \pm 0.010) \times 10^{10}\ s^{-1}\ .$$

4. RARE DECAY MODES

4.1 $\Omega^- \to \Lambda\pi^-$

This decay would violate the $|\Delta S| = 1$ selection rule. A search for canditates has been made using the same procedure as for the $\Omega^- \to \Lambda K^-$ mode with m_{π^-} replacing m_{K^-} in the invariant mass computation. No events were found which satisfied the selection criteria and we set an upper limit on the branching ratio:

$$\frac{\Gamma(\Omega^- \to \Lambda\pi^-)}{\Gamma(\text{all})} < 1.3 \times 10^{-3} \quad \text{at 90\% confidence level.}$$

4.2 $\Omega^- \to \Xi^-\gamma$

The candidate selection has been made in the same way as for the $\Omega^- \to \Xi^-\pi^0$ mode. Additional information on the γ-ray conversion point was provided by a lead/proportional chamber sandwich situated just before the lead-glass array. The remaining background due to the $\Xi^-\pi^0$ mode was eliminated by a cut on the $(\Omega^- - \Xi^-)$ missing mass squared ($m_x^2 < 0$) at the expense of reducing the acceptance for the $\Xi^-\gamma$ decay by a factor of 2. No events have been found and we give an upper limit on the branching ratio:

$$\frac{\Gamma(\Omega^- \to \Xi^-\gamma)}{\Gamma(\text{all})} < 3.1 \times 10^{-3} \quad \text{at 90\% confidence level.}$$

4.3 $\Omega^- \to \Xi^-\pi^+\pi^-$

The search for this decay mode has yielded one clear event with a $\Xi^-\pi^+$ effective mass of 1533 MeV/c^2. The $\Xi^*(1530)\pi$ is expected to dominate the three-body decay mode and, assuming a $\Delta I = \frac{1}{2}$ decay amplitude, the analysed channel

represents four-ninths of all $\Xi^*\pi$ decays. The observed event corresponds to a branching ratio $\Gamma(\Omega^- \to \Xi^*\pi)/\Gamma(\text{all}) \approx 2 \times 10^{-3}$.

4.4 Semi-leptonic decays

We have searched for the decay $\Omega^- \to \Xi^0 e^- \bar{\nu}$ followed by $\Xi^0 \to \Lambda\pi^0$. We have found 4 candidates (3 at 98.5 GeV/c and 1 at 115 GeV/c) which have an electron, identified in the lead-glass and transition radiation counters, and two detected γ-rays which allowed reconstruction of the π^0 and yielded a $\Lambda\pi^0$ mass within ± 10 MeV/c^2 of the Ξ^0 mass. After studying the background from the decays $\Xi^- \to \Lambda\pi^-$, $\Xi^- \to \Lambda(\Sigma^0)e^-\bar{\nu}$, $\Omega^- \to \Lambda K^-$, $\Omega^- \to \Xi^0\pi^-$ and $\Omega^- \to \Xi^-\pi^0$, we estimate the background to be 0.5 events. Three events correspond to a branching ratio $\Gamma(\Xi^0 e^-\bar{\nu})/\Gamma(\text{all}) \simeq 10^{-2}$. A branching ratio of this magnitude is expected from a simple extrapolation of other baryon semi-leptonic decay rates.

5. DISCUSSION AND CONCLUSION

The measured ratio $\Gamma(\Xi^0\pi^-)/\Gamma(\Xi^-\pi^0)$ is 2.94 ± 0.35, while a pure $\Delta I = \frac{1}{2}$ amplitude would have given a ratio of 2.03. Using the QCD framework, a coherent description of the non-leptonic decays of kaons and hyperons has emerged [4]. The elementary operator in the strangeness-changing transition corresponds to the quark scattering process $s + u \to u + d$ in which only one strange quark is involved. The same formalism has been applied to Ω^- decays by Finjord [5]. Because the Ω^- is made of three strange valence quarks, several diagrams which are present for other hyperon decays do not contribute in the Ω^- case. Since the suppressed diagrams correspond to $\Delta I = \frac{1}{2}$ transitions, the relative contribution of $\Delta I = \frac{3}{2}$ is enhanced. The $\Delta I = \frac{3}{2}$ contribution turns out to be 20% of the $\Delta I = \frac{1}{2}$ amplitude, giving a ratio $\Gamma(\Omega^- \to \Xi^0\pi^-)/\Gamma(\Omega^- \to \Xi^-\pi^0) \simeq 3$. This theoretical prediction, which has an uncertainty of about 10%, is in good agreement with our measured ratio.

For the branching ratio $\Gamma(\Omega^- \to \Xi^-\gamma)/\Gamma(\text{all})$ a simple phenomenological model predicts a value of 4.1×10^{-2} [6]. The model assumes that the basic transition

for all radiative weak decays is an s quark decaying into a d quark plus a photon and uses the measured $\Sigma^+ \to p\gamma$ rate as input. Our limit, $\Gamma(\Omega^- \to \Xi^-\gamma)/\Gamma(\text{all}) < 3.1 \times 10^{-3}$ at 90% confidence level, is in clear disagreement with the predicted value.

The results presented have been obtained from about 2400 Ω^- decays. A subsequent Ω^- run with a six-fold increase in statistics has recently been completed. In particular, the analysis of the new data will permit a better measurement of the $\Delta I = 3/2$ contribution to the $\Xi\pi$ decays and provide more detailed information on the $\Xi\pi\pi$ and $\Xi^0 e^- \bar{\nu}$ decay modes.

Table 1

Event numbers, acceptances and branching ratios for the decays $\Omega^- \to \Lambda K^-$, $\Omega^- \to \Xi^0\pi^-$ and $\Omega^- \to \Xi^-\pi^0$. The acceptances given in the table do not include the $\Lambda \to p\pi^-$ branching ratio.

	Beam mom.	Decay modes		
		ΛK^-	$\Xi^0\pi^-$	$\Xi^-\pi^0$
Events	98.5	1208 ± 35	198 ± 15	94 ± 12
	115	712 ± 27	119 ± 11	51 ± 8
Acceptances	98.5	0.519	0.256	0.338
	115	0.637	0.299	0.414
Branching ratios	98.5	0.689 ± 0.017	0.229 ± 0.016	0.082 ± 0.010
	115	0.682 ± 0.021	0.243 ± 0.020	0.075 ± 0.011
$\frac{\Gamma(\Xi^0\pi^-)}{\Gamma(\Xi^-\pi^0)}$	98.5	2.79 ± 0.43		
	115	3.23 ± 0.62		

REFERENCES

[1] M. Bourquin et al., contribution No 776, presented by G. Sauvage, Proc. 19th Int. Conf. High Energy Physics, Tokyo 1978, (Physical Society of Japan, Tokyo, 1979), p. 427.

[2] M. Bourquin et al., submitted to Phys. Letters B.

[3] M. Bourquin et al., Nucl. Phys. B153, 13 (1979).

[4] M.A. Shifman, A.I. Vainshtein and V.I. Zakharov, JETP Lett. 22, 55 (1975); Nucl. Phys. B120, 316 (1977); ITEP preprints 63 and 64 (1975).

[5] J. Finjord, Phys. Lett. 76B, 116 (1978).

[6] F.J. Gilman and M.B. Wise, Phys. Rev. D 19, 976 (1979).

Figure captions

Fig. 1 : $\Omega^- \to \Lambda K^-$ candidates at 98.5 GeV/c:

a) ΛK^- invariant mass, $m_{\Lambda K}$, versus $\Lambda\pi^-$ invariant mass, $m_{\Lambda\pi}$. The cut at $m_{\Lambda\pi} > 1.35$ GeV/c^2 is indicated.

b) $m_{\Lambda K}$ distribution of events with $m_{\Lambda\pi} > 1.35$ GeV/c^2.

Fig. 2 : $m_{\Lambda K}$ versus $(\Omega^- - \pi^-)$ missing mass for $\Omega^- \to \Xi^0\pi^-$ candidates at 98.5 GeV/c.

Fig. 3 : $\Omega^- \to \Xi^0\pi^-$ candidates at 98.5 GeV/c:

a) $(\Xi^0 - \Lambda)$ missing mass, m_x^2, for events with $\Delta p_L > 0.06\ p_{beam}$.

b) $(\Omega^- - \pi^-)$ missing mass for events with $\Delta p_L > 0.06\ p_{beam}$ and -0.03 GeV^2/c^4 $< m_x^2 <$ 0.06 GeV^2/c^4. Shaded area denotes events with no γ signal.

Fig. 4 : $\Omega^- \to \Xi^-\pi^0$ candidates at 98.5 GeV/c:

a) $(\Omega^- - \Xi^-)$ missing mass squared, m_x^2, versus Δp_L. The diagonal cut on Δp_L is indicated.

b) m_x^2 distribution for events with diagonal Δp_L cut applied and with $\Delta p_T > 0.15$ GeV/c. Shaded area denotes events with no γ signal.

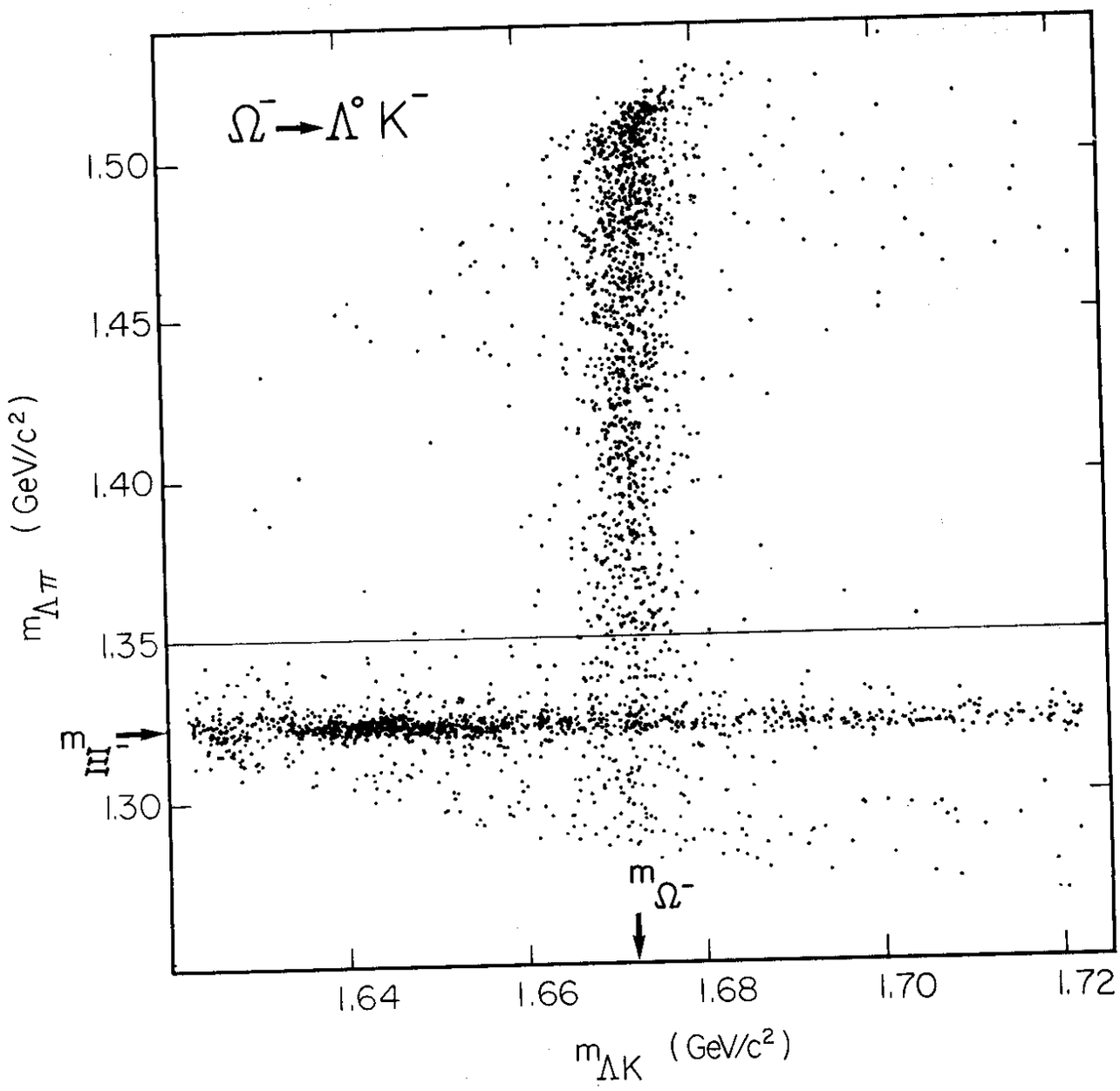
$\Omega^- \rightarrow \Lambda^\circ K^-$
1.50
1.45
1.40
1.35
1.30
$m_{\Lambda\pi}$ (GeV/c²)
m_{Π^-}
m_{Ω^-}
1.64
1.66
1.68
1.70
1.72
$m_{\Lambda K}$ (GeV/c²)

Fig. 1 a)

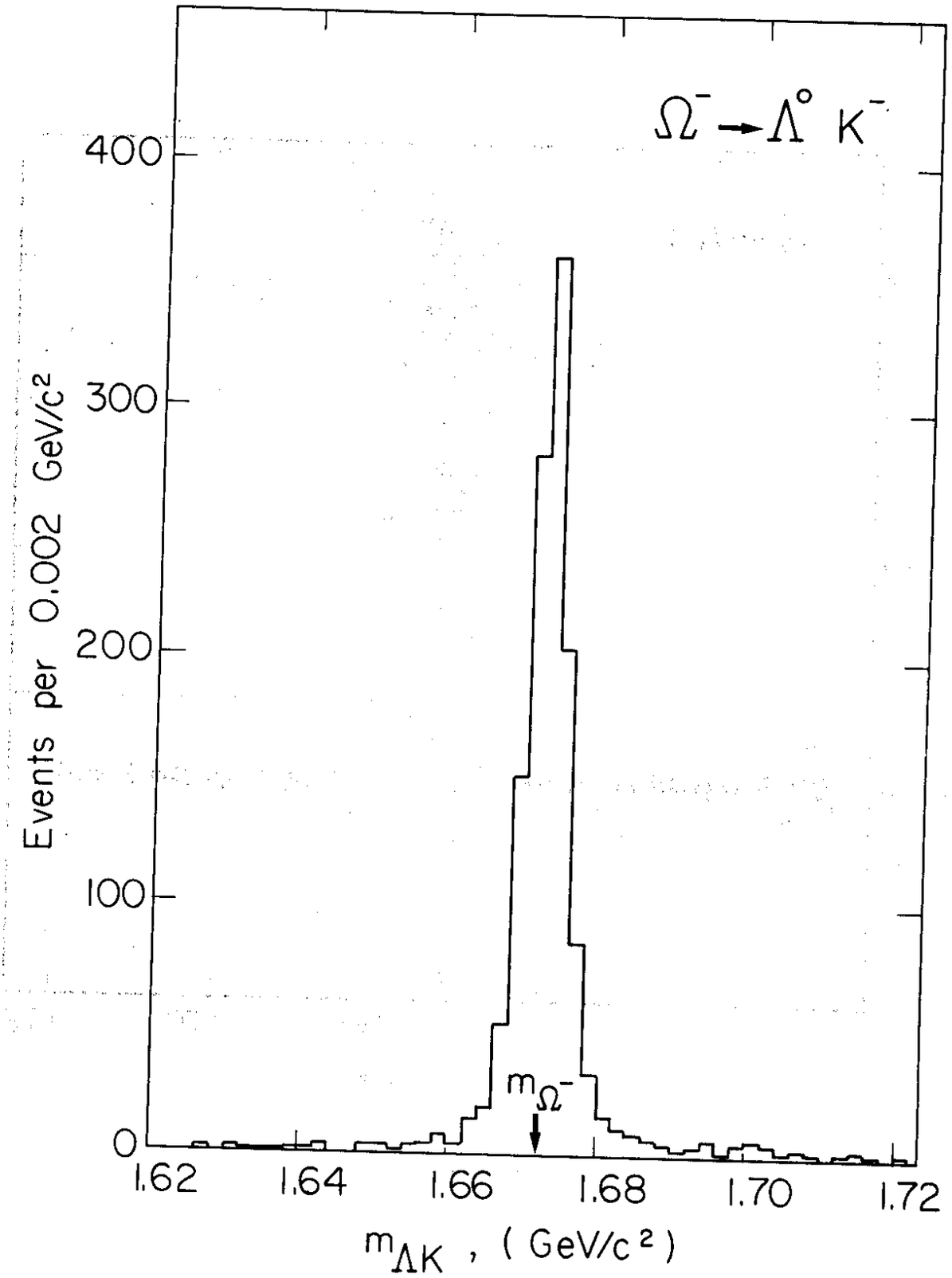
$\Omega^- \rightarrow \Lambda^\circ K^-$
400
300
200
100
0
Events per 0.002 GeV/c²
m_{Ω^-}
1.62
1.64
1.66
1.68
1.70
1.72
$m_{\Lambda K}$, (GeV/c²)

Fig. 1 b)

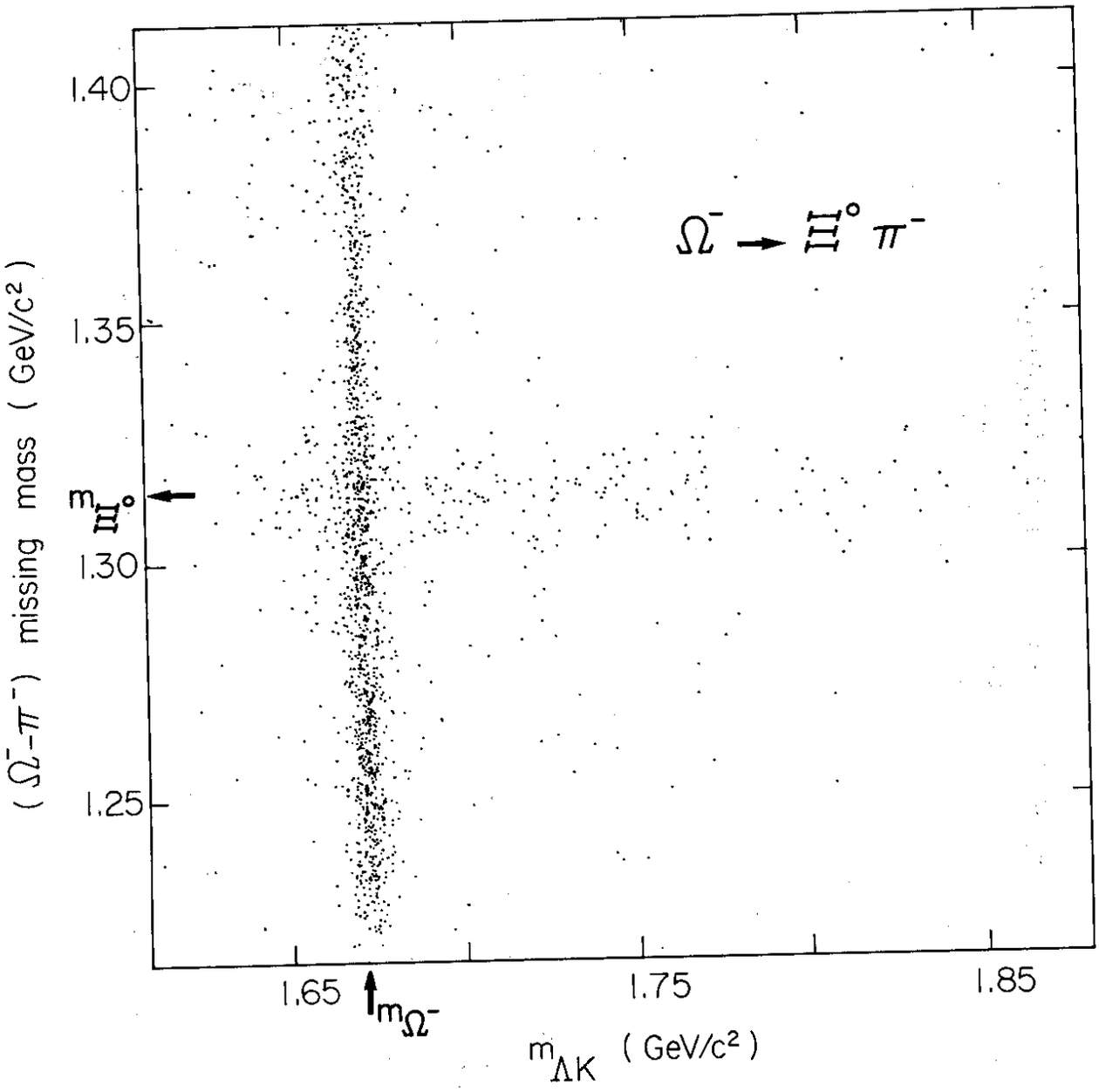
$\Omega^- \rightarrow \Xi^\circ \pi^-$
1.40
1.35
1.30
1.25
m_{Ξ°
$(\Omega^- - \pi^-)$ missing mass (GeV/c^2)
1.65
1.75
1.85
m_{Ω^-}
$m_{\Lambda K}$ (GeV/c^2)

Fig. 2

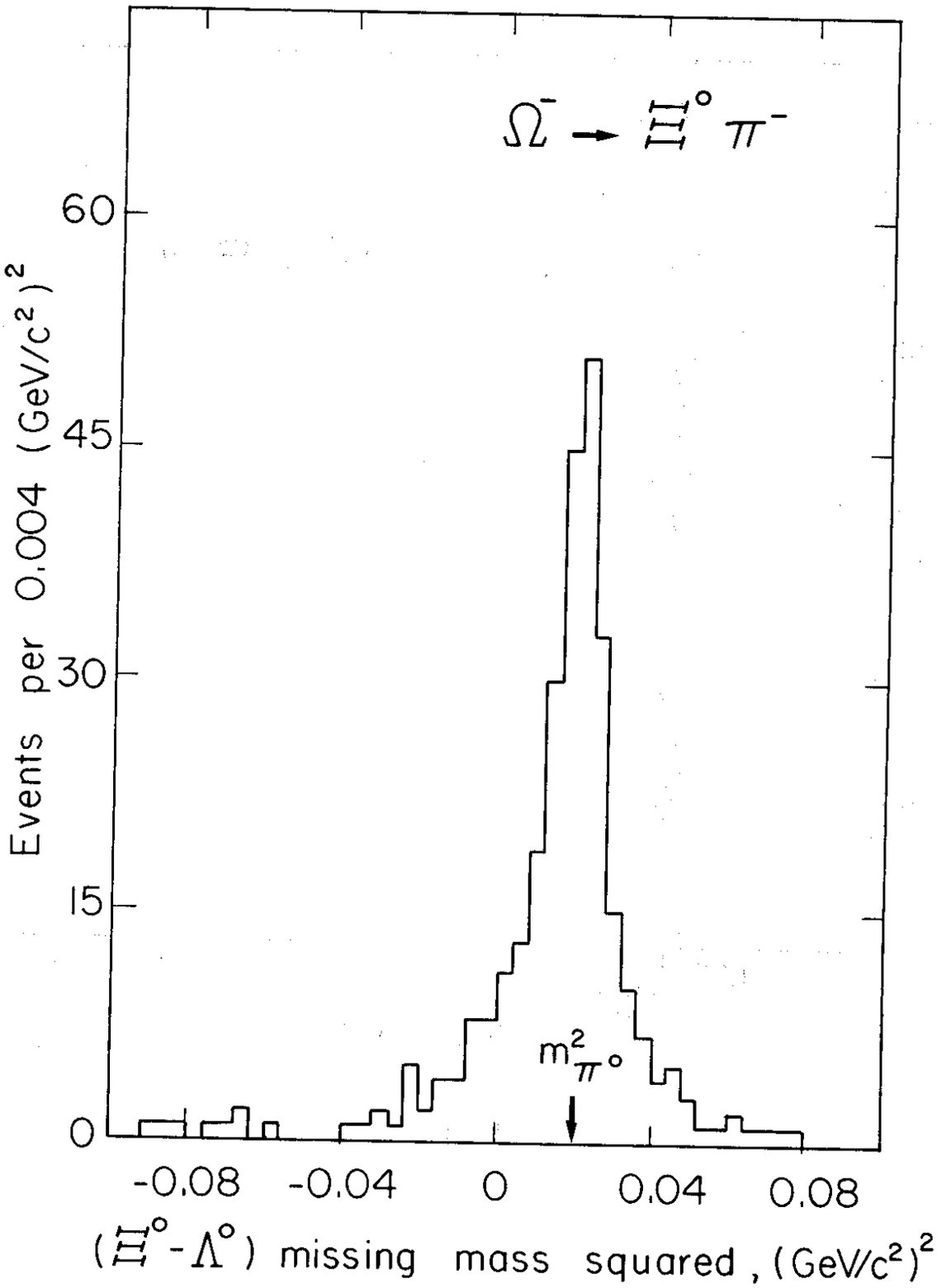
$\Omega^- \rightarrow \Xi^0 \pi^-$
60
45
30
15
0
Events per 0.004 $(GeV/c^2)^2$
$m^2_{\pi^0}$
-0.08
-0.04
0
0.04
0.08
$(\Xi^0 - \Lambda^0)$ missing mass squared, $(GeV/c^2)^2$

Fig. 3 a)

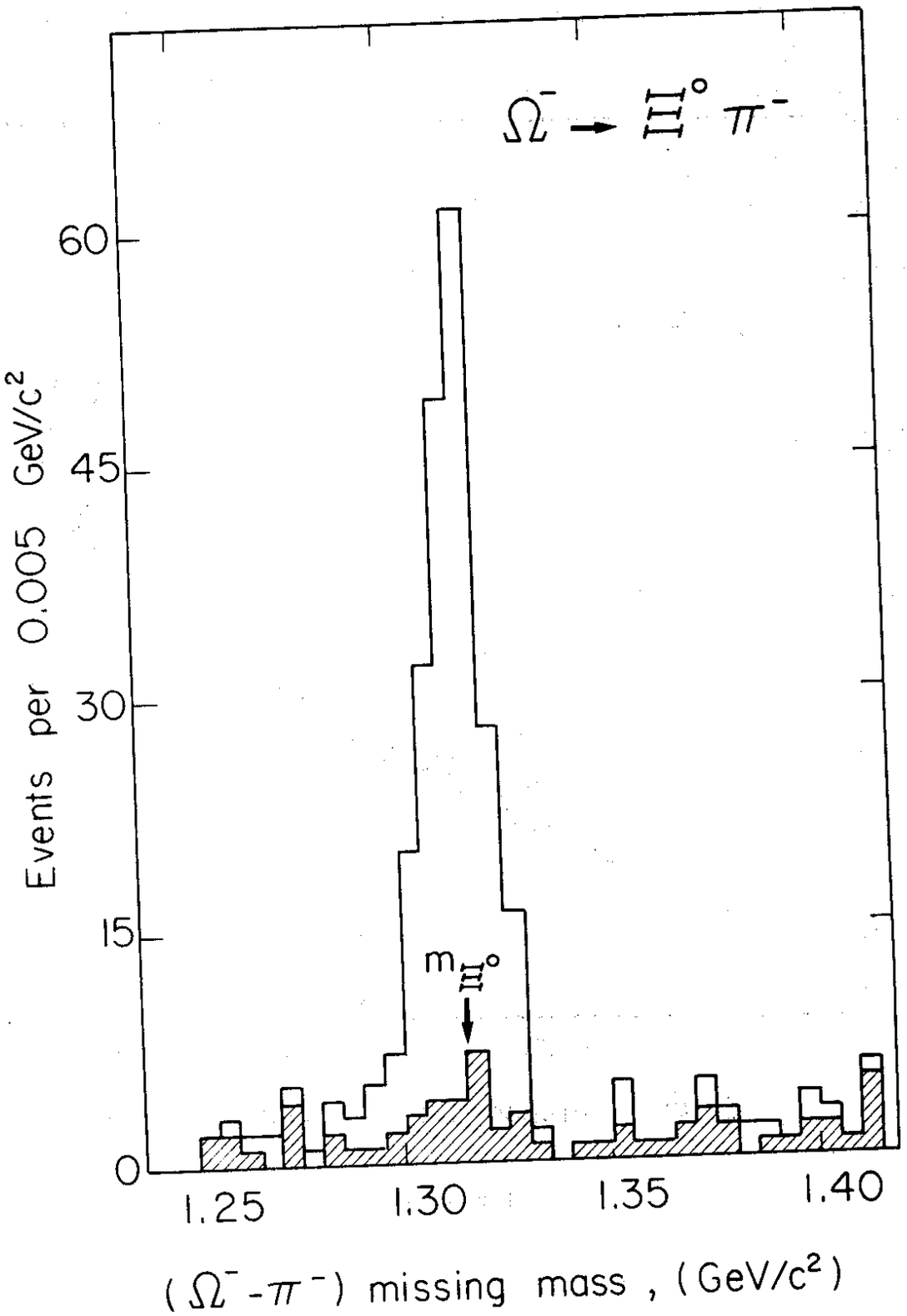
$\Omega^- \rightarrow \Xi^0 \pi^-$
Events per 0.005 GeV/c^2
60
45
30
15
0
m_{Ξ^0}
1.25
1.30
1.35
1.40
($\Omega^- - \pi^-$) missing mass , (GeV/c^2)

Fig. 3 b)

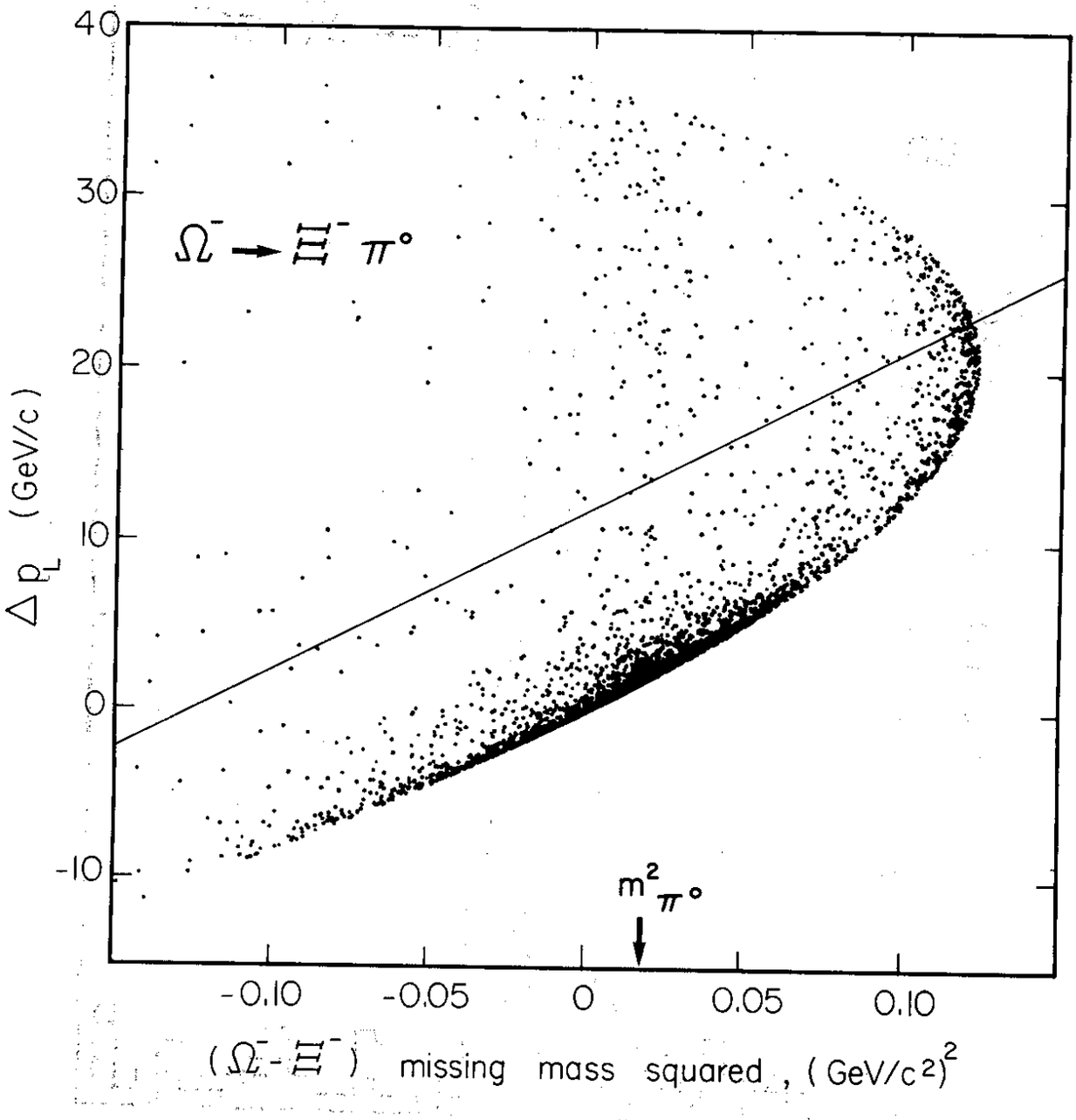
40
30
20
10
0
-10
Δp_L (GeV/c)
$\Omega^- \rightarrow \Xi^- \pi^0$
$m^2_{\pi^0}$
-0.10
-0.05
0
0.05
0.10
$(\Omega^- - \Xi^-)$ missing mass squared, $(GeV/c^2)^2$

Fig. 4 a)

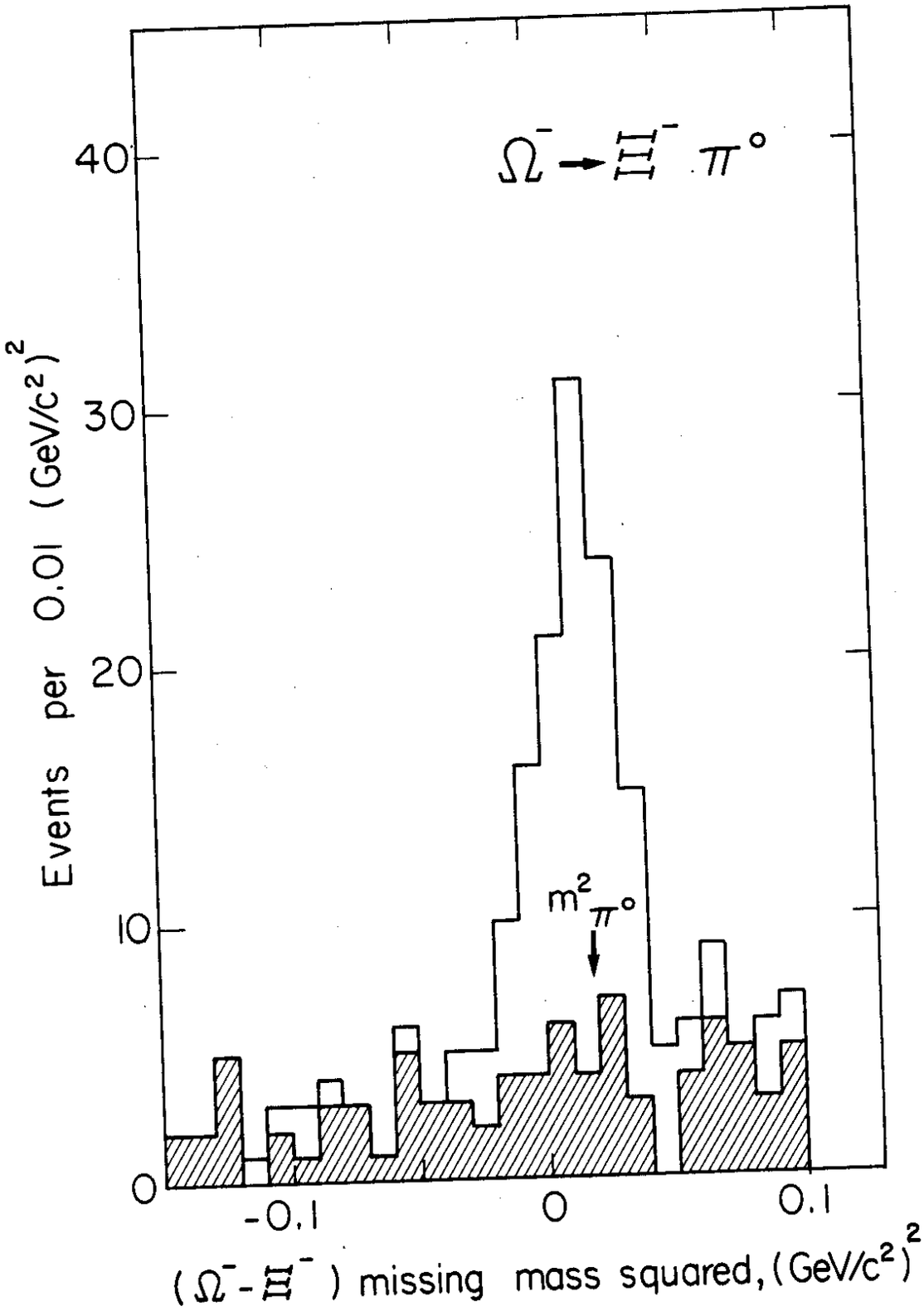
$\Omega^- \rightarrow \Xi^- \pi^0$
Events per 0.01 $(GeV/c^2)^2$
40
30
20
10
0
$m^2_{\pi^0}$
-0.1
0
0.1
$(\Omega^- - \Xi^-)$ missing mass squared, $(GeV/c^2)^2$

Fig. 4 b)